Presentation of Organ Dose and Effective Dose Conversion Factors in Dual-Energy Computed Tomography: A Monte Carlo Simulation Study

Delaram Pakravan (PhD)[1]*

[1]Department of Physics, Ahvaz Branch, Islamic Azad University, Ahvaz, Iran

ABSTRACT

Background: The same conversion factors (*k*-factors) of Single CT (SECT) are applied to estimate the Effective Dose (ED) in Dual Energy Computed Tomography (DECT). However, *k*-factors for different organs need independently validating for DECT, due to the different conditions in DECT.

Objective: This study aimed to calculate organ dose and *k*-factors in different imaging protocols (liver, chest, cardiac, and abdomen) for male and female phantoms.

Material and Methods: This Monte Carlo Simulation study used Monte Carlo N-Particle (MCNP) code for modeling a Siemens Somatom Definition Flash dual-source CT scanner. The organ dose, dose length product, and *k*-factors were calculated for the Medical Internal Radiation Dose (MIRD) of male and female phantoms.

Results: For the male phantom, the *k*-factors for the liver, chest, cardiac, and abdomen-pelvis imaging protocols are equal to 0.020, 0.012, 0.016, and 0.014 mSv. $mGy^{-1}cm^{-1}$, respectively. For the female phantom, the corresponding values are equal to 0.026, 0.023, 0.036, and 0.018, respectively. These values for DECT are different from those corresponding values for SECT, especially for the female phantom.

Conclusion: The calculated *k*-factors for DECT can be used as reference values for the estimation of ED in DECT.

Introduction

Computed Tomography (CT) causes a major radiation dose to patients due to diagnostic radiology examinations. Dual Energy Computed Tomography (DECT) has been proposed as a new approach to more accurately assess human tissues, based on differences in linear attenuation coefficients of human tissues at two energy levels [1-3].

The dual-energy technology leads to increasing concerns about the potential increase in radiation dose received by the patient [4]. However, companies claim that DECT scanning does not have high doses, extensive clinical studies are needed to evaluate this claim for each imaging protocol. Therefore, it is important to measure the radiation dose taken

*Corresponding author:
Delaram Pakravan
Department of Physics, Ahvaz Branch, Islamic Azad University, Ahvaz, Iran
E-mail: dlpakravan69@gmail.com

by patients undergoing DECT, as the assessment of radiation dose should follow the As Low As Reasonably Achievable (ALARA) principle [5]. The effective dose (ED) is the quantity for patient dosimetry. In dosimetry of Single Energy CT (SECT), CT Dose Index (CTDI) is measured in standard phantoms of the head and body. The Dose Length Product (DLP) is calculated by multiplying the volume CTDI ($CTDI_{vol}$) by the scan length, and the effective dose (ED) received by the patient can be determined by multiplying the DLP by a conversion factor (*k*-factor) [1].

The *k*-factors are available for different anatomical regions or imaging protocols for the calculation of the ED in SECT [6]. At present, the same *k*-factors of SECT are used to calculate the ED in the DECT. However, due to the differences between DECT and SECT systems (such as the use of two high and low energies and different fields of view), *k*-factors for different imaging protocols must be independently determined for DECT.

Henzler et al. [7] evaluated the radiation dose related to DECT imaging applications compared to SECT techniques. Ghasemi Shayan et al. [8] discussed the principles of SECT and DECT and their important physical differences, image quality, and CTDI in these two imaging modalities. Ho et al. [9] measured the radiation dose in SECT and DECT imaging for different imaging protocols. Wichmann et al. [10] compared radiation dose and image quality in SECT and DECT abdominal CT protocols. Sabarudin et al. [11] investigated image quality and radiation dose in CT angiography with the use of SECT and DECT. Mazloumi et al. [12] investigated the impact of an iodine Contrast Agent (CA) on radiation dose to organs and tissues during DECT acquisition. Paul et al. [13] determined ED in chest CT for DLP-based and organ dose-based approaches for different protocols in DECT, including high-pitch and second-generation CT scanners. Raudabaugh et al. [14] validated a novel approach to estimate ED in fast-kV switch DECT using Metal Oxide Semiconductor Field-effect Transistor (MOSFET) detectors. The same *k*-factors of SECT or some direct measurement methods were used with limitations for two energies. The CTDI method and *k*-factor were first used for SECT, in which one source is used with a spectrum of energy. In DECT, two sources are used with two different spectrums of energies. Due to gantry limitations, the field of view is different for each source. Therefore, the usable dosimetry methods for the SECT mode may not be suitable for the DECT mode. For this purpose, the MCNP-FBSM MC developed code is applied for DECT dosimetry by calculating the *k*-factor. Thus, it is crucial to steer further studies on different DECT imaging protocols. The Monte Carlo simulation is a widely used method for estimating dosimetric quantities in CT. The purpose of this paper is to use Monte Carlo simulation to calculate organ dose, effective dose, and *k*-factors for various DECT imaging protocols (liver, chest, cardiac, and abdomen) based on male and female phantoms.

Material and Methods

This study is a Monte Carlo Simulation study.

Monte Carlo simulation of the CT scanner

No human participants were involved in this study, and the simulations and calculations were only performed on phantoms. To simulate and validate the CT scanner, a previous study in this field [15] was used as a basis that utilized the MCNP-FBSM (Fan-Beam Source Model) code for data acquisition to simulate a Siemens Somatom Definition Flash (Siemens Healthineers, Erlangen, Germany) dual-source DECT scanner [16]. The developed FBSM Monte Carlo (MC) method was validated for CT dosimetry [17] and also used for the definition of the fan beam. The simulation was performed in the DECT mode in 100 and

140 kVp X-ray energies, which were obtained by a software package based on report number 78 of the Institute of Physics and Engineering in Medicine (IPEM) [18] with a tungsten anode at 7° angle. 3.0 mm Al and 0.9 mm Ti were used for 100 kVp energy as additional filtrations. 3.0 mm Al, 0.9 mm Ti, and 0.4 mm Sn filters were used for 140 kVp energy. In this study, the photon mode was used with an energy cut-off of 100 KeV. To simulate the source motion in the CT, 72 X-ray point sources in 360-degree rotation with 5-degree angular distances were defined around the phantom. F6 tally was used for dose calculation in the simulation code. In MCNPX, the F6 tally values are in terms of MeV/(g.source particle). Then, these values were converted to CTDI in mGy/(100 mAs) using a conversion factor (CF), which is defined as:

$$CF = \frac{CTDI(E,\ ST)_{100,\ air,\ measured\ per\ 100\ mAs}}{CTDI(E,\ ST)_{100,\ air,\ simulated\ per\ particle}} \quad (1)$$

where E and ST are energy and slice thickness, respectively. To validate the simulation, the calculated CTDI values were compared with the corresponding measured values, and a high level of agreement was observed between the CTDI values obtained from the simulation and those obtained from the measurements [15].

Estimate of organ dose and k-factor in DECT mode

Analytical human models were explained in the Oak Ridge National Laboratory (ORNL) publication [19] with the help of analytical equations. All equations and other related data (material compositions, densities, etc.) were defined in the simulation program based on the literature on the Medical Internal Radiation Dose (MIRD) mathematical phantoms [20]. In the present study, the male and female MIRD ORNL phantoms and MCNPX Monte Carlo code [21] were used to evaluate the organ dose. An illustration of the DECT sources and detectors and the MIRD phantom
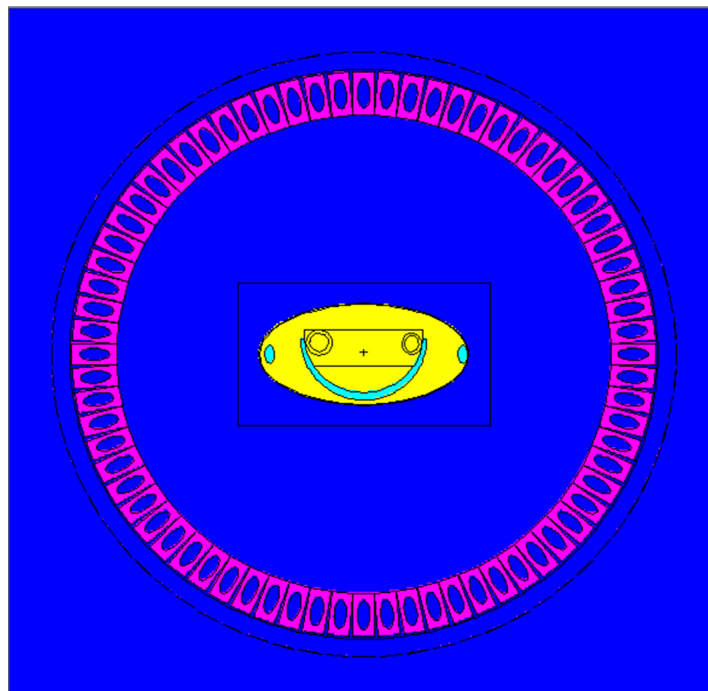
Figure 1: Illustration of the Dual-energy Computed Tomography (DECT) sources and detectors and The Medical Internal Radiation Dose (MIRD) pahntom in the center.

in the center is presented in Figure 1. MIRD male and female phantoms simulated in the MCNPX MC code are illustrated in Figure 2.

After validation and reliability of the simulation code in the previous study [15], the male and female MIRD ORNL phantoms were defined at the center of the DECT gantry, and the organ doses were estimated by applying the following conditions: 100 and 140 kVp tube energies, the pitch of 0.7, and 3.84 cm beam collimation. The scan parameters for liver, chest, cardiac, and abdomen-pelvis imaging protocols for DECT in the simulations of male and female ORNL phantoms are presented in Table 1. These parameters are based on those parameters, which are routinely used in clinics for CT of the mentioned imaging protocols for adult patients. In the simulations, the phantom was moved by 2.688 cm after each tube rotation, and similar irradiation conditions were repeated. After scanning the length of the scan, F6 tally values were summed for different irradiation steps, and the dose of each organ was calculated in terms of mGy/(100 mAs) by the CF. A total of 10^8 particle histories were transported, and the type A percentage uncertainties were less than 5.00%. The MC calculations were done on a Core™ i7 personal computer with a processor of 2.2 GHz and RAM of 16 Gbytes.

ED was calculated using the following formula:

$$ED(Sv) = \sum\nolimits_{T,R} D_{T,R}(Gy) . w_R . w_T \qquad (2)$$

Figure 2: The Medical Internal Radiation Dose (MIRD) phantoms simulated in the MCNPX MC code indicating: male (a) and female (b) phantoms.

Table 1: Scan parameters for liver, chest, cardiac, and abdomen-pelvis imaging protocols for the Dual-Energy Computed Tomography (DECT) in the simulations of the Oak Ridge National Laboratory (ORNL) male and female phantoms

Imaging protocol		Scan start (cm)	Scan end (cm)	Scan length (cm)	Scan length with margin (cm)
Liver	Male	21.50	45.70	24.2	26.89
	Female	21.50	40.32	18.82	21.51
Chest	Male	43.01	69.89	26.88	29.57
	Female	38.10	62.29	24.19	26.88
Cardiac	Male	45.70	56.56	10.86	13.55
	Female	40.79	51.54	10.75	13.44
Abdomen-pelvis	Male	0.00	45.70	45.7	48.39
	Female	0.00	40.32	40.32	43.01

where w_R is the radiation-weighting factor (it is equal to 1.0 for photons), w_T is the tissue-weighting factor, and $D_{T,R}$ is the absorbed dose to tissue T. In this study, the defined weighting factors were used by the International Commission on Radiological Protection (ICRP) report number 103 [22]. Using the ED and DLP, the *k*-factors relevant to liver, chest, cardiac, and abdomen-pelvis imaging protocols for DECT were calculated using the following formula:

$$k\left(\frac{\text{mSv}}{\text{mGy.cm}}\right) = \frac{\text{ED}\,(\text{mSv})}{\text{DLP}\,(\text{mGy.cm})} \qquad (3)$$

where DLP is the product of the CTDI_{vol} and the scan length. The CTDI_{vol} was taken from in-phantom measurements conducted in a previous study for a pitch of 0.7 [15] to calculate the DLP.

Results

Organ dose per 100 mAs (mGy/100 mAs) for liver, chest, cardiac, and abdomen-pelvis imaging protocols were obtained for DECT by simulation of the male and female ORNL phantoms (Table 2). The contribution dose values of different organs for liver, chest, cardiac, and abdomen-pelvis imaging protocols

Table 2: Organ dose per 100 mAs (mGy/100 mAs) for liver, chest, cardiac, and abdomen-pelvis imaging protocols for the dual-energy Computed Tomography (DECT) obtained by simulation of the Oak Ridge National Laboratory (ORNL) male and female phantoms

Organ	Liver		Chest		Cardiac		Abdomen-pelvis	
	Male	Female	Male	Female	Male	Female	Male	Female
Bladder	0.41	0.36	0.12	0.15	0.07	0.09	6.53	6.84
Brain	0.07	0.08	0.22	0.23	0.08	0.09	0.09	0.11
Breast	-	0.76		6.19		5.56	-	1.04
Colon	2.74	2.55	0.20	0.24	0.11	0.14	5.28	5.90
Esophagus	2.08	2.09	3.79	4.45	1.84	2.40	2.17	2.22
Liver	4.79	5.47	1.46	1.98	0.61	0.85	5.05	5.84
Lung	1.90	1.81	5.53	6.18	3.42	4.35	2.04	1.99
Skeleton	3.00	3.00	3.96	5.33	1.76	2.74	5.03	5.67
Skin	1.29	1.17	1.41	1.54	0.58	0.75	2.37	2.46
Stomach	6.22	5.88	0.98	1.24	0.48	0.60	6.55	6.32
Thyroid	0.07	0.13	1.92	2.40	0.10	0.23	0.09	0.17
Adrenals	4.56	5.21	1.69	2.32	0.69	0.93	4.74	5.44
Gall bladder	5.53	5.93	0.49	0.66	0.25	0.36	5.93	6.57
Heart	2.29	1.98	5.62	6.24	4.60	5.31	2.41	2.15
Kidneys	6.00	6.26	0.54	0.67	0.27	0.36	6.36	6.77
Pancreas	5.03	5.28	1.11	1.47	0.57	0.79	5.22	5.57
Small intestine	3.36	2.71	0.21	0.26	0.11	0.15	5.60	6.10
Spleen	5.28	5.31	1.07	1.44	0.51	0.67	5.54	5.65
Thymus	0.57	0.49	7.20	7.11	4.23	4.27	0.68	0.62
Uterus	-	0.65		0.16		0.09	-	6.45
Upper large intestine	0.22	-	0.11	-	0.06		2.40	-

Delaram Pakravan, *et al*

for DECT are presented in Figure 3. In this context, the contribution dose for an organ refers to the fraction of the dose received by that organ about the overall Effective Dose (ED) of the body.

The DLP was obtained using the measured $CTDI_{vol}$ and the scan length. The effective

dose (ED), Dose Length Product (DLP), and k-factors for liver, chest, cardiac, and abdomen-pelvis imaging protocols for DECT were calculated using the reported ED and DLP values. These values, obtained through simulation of the male and female ORNL phantoms, are presented in Table 3, showing for
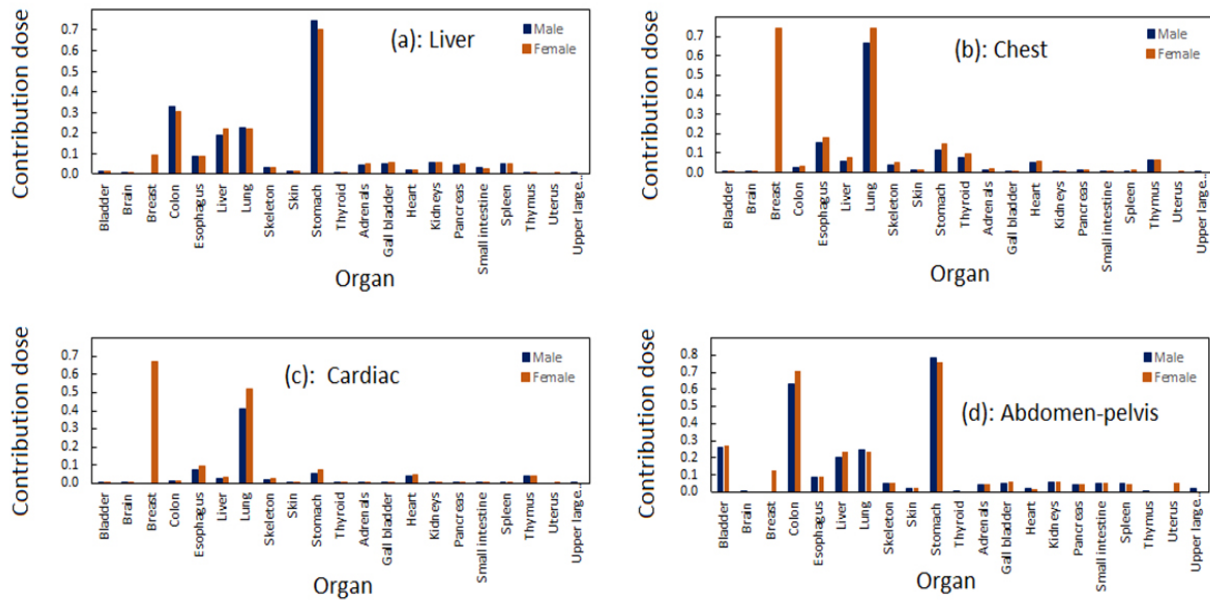
Figure 3: Contribution dose of different organs for liver (a), chest (b), cardiac (c), and abdomen-pelvis (d) imaging protocols for Dual-energy Computed Tomography (DECT)

Table 3: Effective dose per 100 mAs (mSv/100 mAs), The Dose Length Product (DLP) per 100 mAs (mGy.cm/100 mAs) and k-factor (mSv.mGy^{-1}cm^{-1}) for liver, chest, cardiac and abdomen-pelvis imaging protocols for the Dual-energy Computed Tomography (DECT) obtained by simulation of the Oak Ridge National Laboratory (ORNL) male and female phantoms.

Imaging protocol	Effective dose (mSv/100 mAs)		[a]DLP (mGy. cm/100 mAs)		[b]DLP (mGy. cm/100 mAs)		[a]k-factor (mSv. mGy^{-1}cm^{-1})		[b]k-factor (mSv. mGy^{-1}cm^{-1})	
	Male	Female	Male	Female	Male	Female	Male	Female	Male	Female
Liver	1.94	1.99	97.04	75.47	107.83	86.26	0.020	0.026	0.018	0.023
Chest	1.32	2.28	107.79	97.00	118.58	107.79	0.012	0.024	0.011	0.021
Cardiac	0.71	1.57	43.55	43.11	54.34	53.89	0.016	0.036	0.013	0.029
Abdomen-pelvis	2.64	2.92	183.26	161.68	194.04	172.47	0.014	0.018	0.014	0.017

DLP: The dose length product

[a]calculated by the real scan length; [b]calculated by the scan length with margin

the male phantom, the *k*-factors for the liver, chest, cardiac, and abdomen-pelvis imaging protocols are equal to 0.020, 0.012, 0.016, and 0.014 mSv.mGy^{-1}cm^{-1}, respectively. For the female phantom, the corresponding values are equal to 0.026, 0.023, 0.036, and 0.018 mSv.mGy^{-1}cm^{-1}, respectively.

Table 4 presents the organ dose per 100 mAs (mGy/100 mAs) for SECT and DECT for male and female phantoms obtained from this study and other studies for different organs. Table 5 presents the *k*-factors (mSv.mGy^{-1}cm^{-1}) for liver, chest, cardiac, and abdomen-pelvis imaging protocols for SECT and DECT for male and female phantoms obtained from the present study and the study by Christner et al., [6].

Discussion

In the present study, organ dose and ED *k*-factors in different DECT imaging protocols (liver, chest, cardiac, and abdomen) were calculated for male and female phantoms. The *k*-factor is conventionally used for the calculation of ED in CT imaging, dependent on the scanned anatomical region or the imaging protocol. *k*-factors in SECT are ranging between 0.014 and 0.018 mSv.mGy^{-1}cm^{-1} for male and female patients [11]. On the other hand,

Table 4: Organ dose per 100 mAs (mGy/100 mAs) for Single Energy CT (SECT) and the Dual-energy Computed Tomography (DECT) for male and female cardiac protocol from this study and other studies for different organs

Imaging protocol	Cardiac (Present study)		Cardiac (Pakravan et al. [7])	
Organ	Male	Female	Male	Female
Bladder	0.07	0.09	0.26	0.30
Brain	0.08	0.09	0.29	0.33
Breast	-	5.56	-	18.80
Colon	0.11	0.14	0.43	0.48
Esophagus	1.84	2.40	8.11	8.57
Liver	0.61	0.85	2.76	2.85
Lung	3.42	4.35	14.81	15.30
Skeleton	1.76	2.74	7.59	9.70
Skin	0.58	0.75	2.52	2.71
Stomach	0.48	0.60	2.06	2
Thyroid	0.10	0.23	0.46	0.95
Adrenals	0.69	0.93	3.15	3.04
Gall bladder	0.25	0.36	1.08	1.19
Heart	4.60	5.31	18.42	17.8
Kidneys	0.27	0.36	1.17	1.21
Pancreas	0.57	0.79	2.45	2.60
Small intestine	0.11	0.15	.46	0.51
Spleen	0.51	0.67	2.2	2.24
Thymus	4.23	4.27	19.35	18.20
Uterus	-	0.09	-	0.33
Upper large intestine	0.06	-	0.22	-

Table 5: *k*-factor (mSv.mGy^{-1}cm^{-1}) for liver, chest, cardiac and abdomen-pelvis imaging protocols for Single Energy CT (SECT) and the Dual-energy Computed Tomography (DECT) for male and female phantoms from the present study and the study by Christner et al., [6].

Imaging protocol	DECT (Present study)		SECT (Christner et al. [6])		DECT (Christner et al. [6])	
	Male	Female	Male	Female	Male	Female
Liver	0.018	0.023	0.015	0.015	0.017	0.017
Chest	0.011	0.021	0.014	0.014	0.019	0.019
Cardiac	0.013	0.029	0.014	0.014	0.031	0.031
Abdomen-pelvis	0.014	0.017	0.015	0.015	0.016	0.016

DECT: Dual Energy Computed Tomography, SECT: Single Energy CT

based on the results of this study (Table 3), the *k*-factors in DECT for liver, chest, cardiac, and abdomen-pelvis imaging protocols are 0.020, 0.012, 0.016, and 0.014 mSv.mGy^{-1}cm^{-1} for the male phantom and 0.026, 0.023, 0.036, and 0.018 mSv.mGy^{-1}cm^{-1} for the female phantom, respectively. The *k*-factors in DECT for the male phantom are close to the *k*-factors in SECT. For the female phantom, the *k*-factors are different from the male phantom, especially in the cardiac and chest imaging protocols. Therefore, the dose is underestimated if SECT *k*-factors are used for the calculation of the ED in DECT especially for the female patients.

According to the contribution dose results presented in Figure 3, the organs that contribute the most to the overall ED in the cardiac and chest imaging protocols are the breast and lung, while in the liver imaging protocol, the colon, liver, lung, and stomach have the highest share. Similarly, in the abdomen-pelvis imaging protocol, the organs with the highest share of the ED are the bladder, colon, liver, lung, and stomach. The average contribution of the mentioned organs for men and women in the ED is 67%, 57.5%, 75%, and 78% for cardiac, chest, liver, and abdomen-pelvis imaging protocols, respectively. Reducing the dose received by the organs with the highest share to the overall effective dose (ED) is possible by shielding the areas of the body that are not required in the image. However, in this case, the *k*-factor must be recalculated. In a previous study on the field of dosimetry in DECT [15], the same value for the *k*-factor in the cardiac protocol with a pitch of 0.21 was obtained for the male phantom, which was about 12% lower for the female phantom.

The obtained *k*-factors are suitable for patients who have the same anatomies as the phantoms. Using voxel phantoms is more applicable to CT patients compared with those from mathematical phantoms, particularly for the organs with high weighting factors such as bone marrow, breast, lungs, stomach, and colon. ED evaluated with the mathematical phantom is about 40% different from the voxel phantom for head, neck, and abdomen-pelvis imaging protocols [23]. Furthermore, *k*-factors from mathematical phantoms with reference size may underestimate or overestimate the ED [24]. There is currently limited information available regarding the *k*-factors. Rehani et al. [25] emphasized the need to check the accuracy of the displayed dose in different monitoring systems.

While the *k*-factors for the male phantom are similar to the currently used *k*-factors, the *k*-factors are higher for the female phantom. The existing *k*-factor for the chest is similar to the cardiac imaging protocol [11], which may underestimate the ED for female patients. However, taking into account the scan length with the margin results in a slightly lower

k-factor (as shown in Table 3). These values are more accurate if the DLP is recorded on the CT monitor based on the actual scan length.

Table 3 reveals that both the ED and DLP for male and female patients are higher for the abdomen-pelvis imaging protocol compared to the other imaging protocols. This may be attributed to the higher sensitivity of the organs located in the abdomen-pelvis region compared to the other organs in the vicinity of the other imaging protocols. As shown in Table 2 for different imaging protocols, organs located inside the radiation field received higher doses compared to other organs. In other words, organs receiving the primary radiation had higher organ doses. Additionally, organs close to the radiation field also had higher doses compared to other organs.

Table 4 reveals that the organ doses are different in the present study and others that may be due to differences in the X-ray energy, phantom type, and imaging conditions. Also, Table 5 shows k-factors are different between SECT and DECT. Additionally, there are differences between the data for k-factors from the present study and the study by Christner et al. [6] for DECT. While in the study by Christner et al. [6], there is no difference in k-factors observed between males and females in the present study, a different trend was in the data for males and females. The varying conditions in the two studies affect the results.

Henzler et al. [7] evaluated the radiation dose related to DECT compared to SECT techniques and concluded that DECT imaging with DSCT does not have a high radiation dose. However, the radiation dose from the other approaches of DECT must be evaluated. Ghasemi Shayan et al. [8] discussed the principles of SECT and DECT and their important physical differences and also different organs in terms of image quality and CTDI in these two imaging modalities. Based on their results, the image quality and their dose amount should be compared in two imaging modalities due to various data and statistics. Ho et al.

[9] measured the radiation dose in SECT and DECT imaging for adult liver, renal, and aortic imaging protocols and also concluded that radiation doses from DECT imaging were higher than those from SECT imaging for the evaluated abdominal imaging protocols. Wichmann et al. [10] compared radiation dose and image quality in SECT and DECT abdominal CT protocols and their results showed that DECT did not result in higher radiation dose exposure or differences in image quality compared to SECT. Sabarudin et al. [11] compared the image quality and radiation dose of CT angiography using SECT and DECT, and showed the lower radiation doses in prospective ECG-triggered CCTA. Mazloumi et al. [12] investigated the impact of iodine CA on radiation dose to organs and tissues during DECT acquisition and presented that the use of CA in DECT led to an average organ dose increase of 30%. Paul et al. [13] determined ED during standard chest CT for organ dose-based and DLP-based approaches for four different scan protocols in DECT, including a high-pitch and second-generation CT scanner. ED values by ICRP 103 and 60 phantoms for both SECT and DECT imaging examinations did not differ more than 0.04 mSv. In the current study, both male and female phantoms were considered, and the k-factors were separately obtained for male and female phantoms. Table 3 shows the k-factors related to male and female phantoms are different. The k-factor for chest protocol (0.014 or 0.017 mSv.mGy^{-1}cm^{-1}) is currently applied to estimate the cardiac imaging ED [11], significantly underestimating the ED for female patients. The DECT with effective mAs of 89/76 was applied on tubes with 100 kV/Sn 140 kV with a pitch of 0.55 for the chest imaging with a 49 cm scan length [15]. In this study, the effective mAs were calculated as 38/33 and 35/30 for the chest imaging protocol, 16/13 and 15/13 for the cardiac imaging protocol, 35/30 and 27/23 for the liver imaging protocol, and 65/56 and 58/49 for the abdomen imaging protocol used for the male

004

Delaram Pakravan, *et al*

and female phantoms, respectively. The mean ED was 0.93 mSv and 1.48 mSv for the chest imaging protocol, 0.21 mSv and 0.44 mSv for the cardiac imaging protocol, 1.26 mSv and 0.99 mSv for the liver imaging protocol, and 3.20 mSv and 3.13 mSv for the abdomen imaging protocol for male and female ORNL phantoms, respectively.

Additional simulations could be performed using different DECT imaging protocols and simulation codes to enhance the reliability of the results and decrease the level of uncertainty. In addition, the MIRD phantoms utilized in this study contain certain geometric simplifications. More phantoms, such as the ICRP 110 phantoms, should be evaluated due to the absence of specific organ definitions, such as salivary glands and red bone marrow in the MIRD phantoms. A phantom placed in the center of the gantry was used in the simulations, while the sick person may not be placed in the center of the gantry. Therefore, the related uncertainties as Size-specific Dose Estimation (SSDE) should be investigated.

Conclusion

The MCNP-FBSM MC developed code is a beneficial tool with reliable results for DECT dosimetry. The results indicate that the DECT k-factors obtained in this study differ from both the SECT k- and DECT k-factors reported in the literature. Moreover, the k-factors were dissimilar between males and females. In the liver, chest, cardiac, and abdomen-pelvis DECT protocols, the k-factor in the female phantom is higher than the male phantom and is also significant for chest and cardiac protocols. Therefore, the use of the male k-factor for DECT imaging protocol will result in underestimating the ED for female patients. There are limited studies to estimate dose in DECT mode. Therefore, empirical measurements and simulations are offered for all imaging protocols to reduce the related uncertainties and increase the reliability of the organ dose and ED results in DECT. It is crucial to conduct

research on DECT dosimetry and to determine all necessary dosimetry factors, such as CTDI, DLP, SSDE, and k-factor for various imaging protocols.

Ethical Approval

This study was conducted under the ethical protocols of Islamic Azad University (Ahvaz Branch). No animal or human participants were involved in this study, and only CT dosimetric data were analyzed.

Conflict of Interest

None

References

1. McCollough C, Cody D, Edyvean S, Geise R, Gould B, Keat N, et al. The measurement, reporting, and management of radiation dose in CT. Report of AAPM Task Group 23. American Association of Physicists in Medicine One Physics Ellipse; 2008.

2. Valentin J, International Commission on Radiation Protection. Managing patient dose in multidetector computed tomography(MDCT). ICRP Publication 102. *Ann ICRP*. 2007;**37**(1):1-79. doi: 10.1016/j.icrp.2007.09.001. PubMed PMID: 18069128.

3. Smith-Bindman R, Lipson J, Marcus R, Kim KP, Mahesh M, Gould R, et al. Radiation dose associated with common computed tomography examinations and the associated lifetime attributable risk of cancer. *Arch Intern Med.* 2009;**169**(22):2078-86. doi: 10.1001/archinternmed.2009.427. PubMed PMID: 20008690. PubMed PMCID: PMC4635397.

4. Roele ED, Timmer VCML, Vaassen LAA, Van Kroonenburgh AMJL, Postma AA. Dual-Energy CT in Head and Neck Imaging. *Curr Radiol Rep.* 2017;**5**(5):19. doi: 10.1007/s40134-017-0213-0. PubMed PMID: 28435761. PubMed PMCID: PMC5371622.

5. Lyu T, Zhao W, Zhu Y, Wu Z, Zhang Y, Chen Y, et al. Estimating dual-energy CT imaging from single-energy CT data with material decomposition convolutional neural network. *Med Im-*

age Anal. 2021;**70**:102001. doi: 10.1016/j.media.2021.102001. PubMed PMID: 33640721.

6. Christner JA, Kofler JM, McCollough CH. Estimating effective dose for CT using dose-length product compared with using organ doses: consequences of adopting International Commission on Radiological Protection publication 103 or dual-energy scanning. *AJR Am J Roentgenol.* 2010;**194**(4):881-9. doi: 10.2214/AJR.09.3462. PubMed PMID: 20308486.

7. Henzler T, Fink C, Schoenberg SO, Schoepf UJ. Dual-energy CT: radiation dose aspects. *AJR Am J Roentgenol.* 2012;**199**(5 Suppl):S16-25. doi: 10.2214/AJR.12.9210. PubMed PMID: 23097163.

8. Ghasemi Shayan R, Oladghaffari M, Sajjadian F, Fazel Ghaziyani M. Image Quality and Dose Comparison of Single-Energy CT (SECT) and Dual-Energy CT (DECT). *Radiol Res Pract.* 2020;**2020**:1403957. doi: 10.1155/2020/1403957. PubMed PMID: 32373363. PubMed PMCID: PMC7189324.

9. Ho LM, Yoshizumi TT, Hurwitz LM, Nelson RC, Marin D, Toncheva G, Schindera ST. Dual energy versus single energy MDCT: measurement of radiation dose using adult abdominal imaging protocols. *Acad Radiol.* 2009;**16**(11):1400-7. doi: 10.1016/j.acra.2009.05.002. PubMed PMID: 19596594.

10. Wichmann JL, Hardie AD, Schoepf UJ, Felmly LM, Perry JD, Varga-Szemes A, et al. Single- and dual-energy CT of the abdomen: comparison of radiation dose and image quality of 2nd and 3rd generation dual-source CT. *Eur Radiol.* 2017;**27**(2):642-50. doi: 10.1007/s00330-016-4383-6. PubMed PMID: 27165140.

11. Sabarudin A, Sun Z, Yusof AK. Coronary CT angiography with single-source and dual-source CT: comparison of image quality and radiation dose between prospective ECG-triggered and retrospective ECG-gated protocols. *Int J Cardiol.* 2013;**168**(2):746-53. doi: 10.1016/j.ijcard.2012.09.217. PubMed PMID: 23098849.

12. Mazloumi M, Van Gompel G, Kersemans V, De Mey J, Buls N. The presence of contrast agent increases organ radiation dose in contrast-enhanced CT. *Eur Radiol.* 2021;**31**(10):7540-9. doi: 10.1007/s00330-021-07763-7. PubMed PMID: 33783569. PubMed PMCID: PMC8452580.

13. Paul J, Banckwitz R, Krauss B, Vogl TJ, Maentele W, Bauer RW. Estimation and comparison of effective dose (E) in standard chest CT by organ dose measurements and dose-length-product methods

and assessment of the influence of CT tube potential (energy dependency) on effective dose in a dual-source CT. *Eur J Radiol.* 2012;**81**(4):e507-12. doi: 10.1016/j.ejrad.2011.06.006. PubMed PMID: 21703793.

14. Raudabaugh J, Nguyen G, Lowry C, Januzis N, Colsher J, Nelson R, Yoshizumi TT. Effective dose estimation from organ dose measurements in fast-kV switch dual energy computed tomography. *Radiat Prot Dosimetry.* 2018;**182**(3):352-8. doi: 10.1093/rpd/ncy072. PubMed PMID: 30590847.

15. Pakravan D, Babapour Mofrad F, Deevband MR, Ghorbani M, Pouraliakbar H. Organ dose in cardiac dual-energy computed tomography: a Monte Carlo study. *Phys Eng Sci Med.* 2022;**45**(1):157-66. doi: 10.1007/s13246-021-01098-9. PubMed PMID: 35015205.

16. Khodajou-Chokami H, Hosseini SA, Ay MR, Zaidi H. MCNP-FBSM: Development of MCNP/MCNPX source model for simulation of multi-slice fan-beam x-ray CT scanners. International Symposium on Medical Measurements and Applications (MeMeA); Istanbul, Turkey: IEEE; 2019.

17. Pakravan D, Babapour Mofrad F, Deevband MR, Ghorbani M, Pouraliakbar H. A Monte Carlo Platform for Characterization of X-Ray Radiation Dose in CT Imaging. *J Biomed Phys Eng.* 2021;**11**(3):271-80. doi: 10.31661/jbpe.v0i0.2012-1254. PubMed PMID: 34189115. PubMed PMCID: PMC8236108.

18. Cranley K, Gilmore BJ, Fogarty GWA, Deponds L. Catalog of diagnostic X-ray spectra and other data. IPEM report no. 78; IPEM Publications; 1997.

19. Stabin M, Watson E, Cristy M, Ryman J, Eckerman K, Davis J, et al. Mathematical models and specific absorbed fractions of photon energy in the nonpregnant adult female and at the end of each trimester of pregnancy. ORNL Report ORNL/TM-12907; Tennessee: Oak Ridge National Laboratory; 1995. Avaailable from: https://digital.library.unt.edu/ark:/67531/metadc791641/m2/1/high_res_d/91944.pdf.

20. Krstić D, Nikezić D. Input files with ORNL-mathematical phantoms of the human body for MCNP-4B. *Comput Phys Commun.* 2007;**176**(1):33-7. doi: 10.1016/j.cpc.2006.06.016.

21. Waters LS. MCNPX User's Manual, Version 2.3.0. Report LA-CP-02-408; Los Alamos National Laboratory; 2002. Avaailable from: https://mcnpx.lanl.gov/pdf_files/TechReport_2002_LANL_LA-

UR-02-2607_Waters.pdf.

22. The 2007 Recommendations of the International Commission on Radiological Protection. ICRP publication 103. *Ann ICRP.* 2007;**37**(2-4):1-332. doi: 10.1016/j.icrp.2007.10.003. PubMed PMID: 18082557.

23. Lee C, Flynn MJ, Judy PF, Cody DD, Bolch WE, Kruger RL. Body Size-Specific Organ and Effective Doses of Chest CT Screening Examinations of the National Lung Screening Trial. *AJR Am J Roentgenol.* 2017;**208**(5):1082-8. doi: 10.2214/AJR.16.16979. PubMed PMID: 28267354.

24. Huda W, Ogden KM, Khorasani MR. Converting dose-length product to effective dose at CT. *Radiology.* 2008;**248**(3):995-1003. doi: 10.1148/radiol.2483071964. PubMed PMID: 18710988. PubMed PMCID: PMC2657852.

25. Rehani MM, Yang K, Melick ER, Heil J, Šalát D, Sensakovic WF, Liu B. Patients undergoing recurrent CT scans: assessing the magnitude. *Eur Radiol.* 2020;**30**(4):1828-36. doi: 10.1007/s00330-019-06523-y. PubMed PMID: 31792585.